Макрогетероциклы
http://mhc-isuct.ru

DOI: 10.6060/mhc224864s

Aluminum Phthalocyanine – [60]Fullerene Supramolecular Dyads: Synthesis, Photophysical Properties and ROS Photogeneration

Lev R. Sizov,[a@] Daria V. Revina,[a,b] Alexander Yu. Rybkin,[a] Alexei V. Kozlov,[a] Anatoliy P. Sadkov,[a] and Nikolay S. Goryachev[a,b]

[a]*Federal Research Center of Problems of Chemical Physics and Medicinal Chemistry RAS, 142432 Chernogolovka, Russia*
[b]*Lomonosov Moscow State University, 119991 Moscow, Russia*
[@]*Corresponding author E-mail: Leo.Sizoff@yandex.ru*

An axially substituted aluminum phthalocyanine–[60]fullerene derivative supramolecular dyads have been prepared. For the first time, such structures were evaluated as the type I photosensitizers for photodynamic therapy (PDT). Compared to the native dye, the fluorescence in the obtained compounds is partially quenched and efficiency of singlet oxygen production is reduced. The dyad aluminum phthalocyanine–phenyl-C_{60}-butyric acid encapsulated in polyvinylpyrrolidone nanoparticles showed a threefold increase in the superoxide anion-radical generation compared to the native dye, which indicates the promising potential of this dyad as a type I photosensitizer for PDT.

Keywords: Aluminum phthalocyanine, fullerene derivatives, supramolecular dyad, mass spectrometry, fluorescence quantum yield, photochemical activity, superoxide generation.

Диады фталоцианин алюминия–[60]фуллерен: Синтез, фотофизические свойства и фотогенерация АФК

Л. Р. Сизов,[a@] Д. В. Ревина,[a,b] А. Ю. Рыбкин,[a] А. В. Козлов,[a] А. П. Садков,[a] Н. С. Горячев[a,b]

[a]*Федеральный исследовательский центр проблем химической физики и медицинской химии РАН, 142432 Черноголовка, Россия*
[b]*Московский государственный университет им. М.В. Ломоносова, 119991 Москва, Россия*
[@]*E-mail: Leo.Sizoff@yandex.ru*

Через аксиальное замещение были получены супрамолекулярные диады на основе фталоцианина алюминия и производных фуллерена. Впервые такие структуры были оценены как фотосенсибилизаторы I типа для использования в фотодинамической терапии. По сравнению с исходным красителем в полученных диадах происходит частичное тушение флуоресценции и снижение эффективности генерации синглетного кислорода. Инкапсулированная в наночастицы поливинилпирролидона диада фталоцианин алюминия–фенил-C_{60}-масляная кислота генерировала супероксид анион-радикал в три раза сильнее, чем исходный краситель, что показывает перспективность данной диады в качестве фотосенсибилизатора I типа для ФДТ.

Ключевые слова: Фталоцианин алюминия, производные фуллерена, супрамолекулярная диада, масс-спектрометрия, квантовый выход флуоресценции, фотохимическая активность, генерация супероксида.

Intoduction

In recent years, Type I photosensitizers for photodynamic therapy (PDT) have attracted increasing interest from researchers all over the world.[1,2] Such photosensitizers are able to generate superoxide radical $O_2^{\bullet-}$, hydrogen peroxide H_2O_2, hydroxyl radical $HO^{\bullet}$ and/or non-oxygen free radicals under light irradiation. Type I photochemical reactions are significantly less dependent on the concentration of oxygen in the medium than the Type II mechanism

which involves singlet oxygen photogeneration. In addition, the hydroxyl radical HO• is considered to be more cytotoxic than $^1O_2$.[3]

Type I mechanism of photodynamic action was shown for inorganic (metal oxides,[4] carbon nanomaterials[5]), organic[6] and hybrid[7] nanomaterials. The same applies to different small molecules such as methylene blue derivatives, boron-dipyrromethanes (BODIPY) dyes, complexes of transition metals with macroheterocycles and other organic ligands.[2] Unfortunately, only a small number of such structures meet the extensive list of PDT drug requirements: biocompatibility, low dark toxicity, strong light absorption in the red/near-infrared (NIR) region, so-called «tissue transparency window» *etc*.

One of the promising approaches to the creation of biocompatible Type I photosensitizers is the use of organic donor-acceptor structures. They do not contain heavy metals and are capable of forming the long-lived charge transfer (CT) state upon irradiation. In particular, in such structures, [60]fullerene can act as an efficient electron acceptor, and a dye that absorbs in the red/NIR region can act as a donor.[8] Due to the rigid structure, fullerene has a low reorganization energy of electron transfer, which favors the formation of the long-lived CT state in donor-acceptor dyads.[9] It has been reported that porphyrin-C_{60} dyad forming photoinduced CT state retained a high phototoxic activity toward cancer cells even under hypoxic conditions.[10] We have previously detected an increase in $O_2^{\bullet-}$ formation compared with the original dye in the cases of non-covalent xanthene dye–C_{60} dyad[11] and covalent dyads based on fullerene and dyes ruboxyl,[12] pyropheophorbide[13] and chlorin e_6.[14]

From this point of view, phthalocyanine and its derivatives are highly attractive for the creation of such fullerene-dye dyads. Phthalocyanines have successfully proven themselves as photochemically stable Type II photosensitizers in PDT of malignant tumors.[15-18] Phthalocyanines can act as efficient donors in photoinduced electron transfer due to their readily ionizable π-electron system and as red/NIR dye antennas.[19]

To obtain a stable fullerene–dye dyad, a number of studies have used axial coordination between a metal ion in the phthalocyanine and the fullerene derivative. For example, a supramolecular coordination of pyrrolidinofullerenes and zinc phthalocyanine is often used for that purpose.[20-24] Titanium (IV),[25] silicon,[26] manganese(III),[27] and other metals can also be applied for the axial coordination of pyrrolidinofullerenes to the central metal ions in the phthalocyanine. Nevertheless, we have not found any data in the literature on testing such complexes as Type I photosensitizers for PDT.

Thus, the present work aimed to obtain donor–acceptor dyads formed by axial coordination of aluminum phthalocyanine and monosubstituted fullerene derivatives and study their photophysical and photochemical properties as Type I photosensitizers for PDT.

Experimental

General

Chemicals. Phthalonitrile, aluminum chloride hexahydrate, DPBF (1,3-diphenylisobenzofuran), NADH (nicotinamide adenine dinucleotide), NBT (nitro blue tetrazolium chloride), EDTA (ethylenediaminetetraacetic acid) were purchased from Sigma-Aldrich. Chlorobenzene and silica gel (40–60 μm, 60 Å) were purchased from Acros organics. Fullerene C_{60} (99.5%) was purchased from Fullerene Center, Nizhny Novgorod. Other reagents and solvents were used without further purification.

Equipment for chemical characterization. Matrix-assisted laser desorption/ionization time-of-flight (MALDI-TOF) mass spectra were taken on a Bruker Autoflex II mass spectrometer with 2,5-dihydroxybenzoic acid as the matrix.

Synthesis

Precursors of supramolecular dyads were synthesized by the described methods: aluminum phthalocyanine chloride **PcAl**,[28] cyclopropane fullerene derivative – phenyl-C_{60}-butyric acid (**I**)[29] – for dyad **III** and pyrrolidinofullerene – C_{60}-substituted benzoic acid (**II**)[30] – for dyad **IV**.

*Supramolecular dyads **III** and **IV*** (Figure 1). Aluminum phthalocyanine chloride (1 eqv) and corresponding fullerene derivatives (1 eqv) were dissolved in a mixture of pyridine/chlorobenzene (1:1, vol/vol). The reaction mixture was boiled with continuous stirring for 6 hours. After completion of the reaction, the solvent was removed under reduced pressure, the product was isolated by gel permeation chromatography (Bio-Beads S-X1, Bio-Rad) in pyridine. For dyad **III** found C 84.828, H 1.896, N 8.575 % (calculated for $C_{102}H_{26}N_9O_2Al$: C 85.292, H 1.825, N 8.777 %). For dyad **IV** found C 85,703, H 1.967, N 7.822 %, (calculated for $C_{103}H_{27}N_8O_2Al$: C 86.188, H 1.896, N 7.807 %). MS(MALDI-TOF): *m/z* = 1436 $[M+H]^-$, calculated for $C_{103}H_{28}N_8O_2Al$ 1436 (dyad **III**); *m/z* = 1437 $[M+H]^+$, calculated for $C_{102}H_{27}N_9O_2Al$ 1437 (dyad **IV**).

Solubilization of compounds under study in the water with polyvinylpyrrolidone. To evaluate superoxide anion generation in water solution, hydrophobic compounds – the reference dye and dyads – were encapsulated into nanoparticles of polyvinylpyrrolidone (PVP, Mr ~ 45000, Sigma) using a modified procedure for dissolving native fullerene C_{60} in water.[31] The compound under study was dissolved in pyridine, and a solution of PVP in pyridine was added (compound under study/PVP = 1:10, mol/mol).

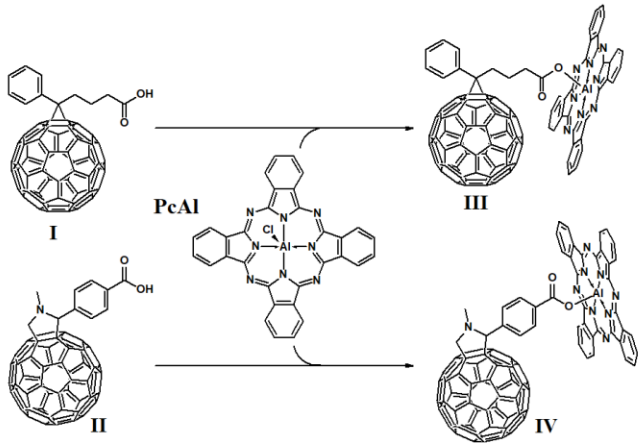

Figure 1. Synthesis of PcAl–C_{60} dyads **III** and **IV**.

Pyridine was removed on a rotary evaporator. The residue was redissolved in 3-5 mL of water using an ultrasonic bath, and then the water was also removed on a rotary evaporator to completely remove traces of pyridine. Then, water was added again to achieve 0.1 mM compound concentration. The hydrodynamic radius of the obtained nanoparticles in an aqueous solution was measured by the previously described dynamic light scattering (DLS) method.[14]

Photophysical Studies

Absorption spectra were measured using a Cary-60 spectrophotometer equipped with a thermostated cell. Fluorescence steady-state spectra were recorded by a Cary-Eclipse fluorescence spectrophotometer. Fluorescence quantum yields of the compounds under study were calculated using chlorin e_6 trisodium salt as a reference (Φ_{fl} = 15% in ethanol[32]) according to the formula:

$$\Phi_i = \frac{(1-10^{-A_{ref}})}{(1-10^{-A_i})} \frac{n_i^2}{n_{ref}^2} \frac{\alpha_i}{\alpha_{ref}} \Phi_{ref} , \quad (1)$$

where A_i and A_{ref} are absorption intensities at the excitation wavelength, n_i and n_{ref} are refractive indexes of the medium, α_i and α_{ref} are areas under the fluorescence spectrum for the compound under study and reference compound respectively.

Photochemical Studies

Detection of singlet oxygen $^1O_2$ formation has been done by a standard method using 1,3-diphenylisobenzofuran (DPBF) probe.[33] The cuvette with the pyridine solution of the compound under study and DPBF (50 μM) was illuminated by a setup based on a Specord M-40 spectrophotometer equipped with an interface for computer recording of spectra, a temperature-controlled cell compartment (set to 20 °C) with integrated LEDs (λ = 660 nm, radiation power = 5 mW), and an Arduino-based control unit. The absorbance decrease of the DPBF probe was registered every 2 s of light exposure at 420 nm. Singlet oxygen quantum yields of the compounds under study were calculated using zinc phthalocyanine as a reference (Φ_Δ = 40% in DMSO[34]) according to the formula:

$$\Phi_\Delta^i = \frac{\alpha^{ref}}{\alpha^i} \frac{k^i}{k^{ref}} \Phi_\Delta^{ref} \quad (2)$$

where α^i and α^{ref} are areas under the absorbance spectrum (taking into account the emission spectrum of the photoexcitation source), k^i and k^{ref} are reaction rate constants for photobleaching of 1,3-diphenylisobenzofuran for the compound under study and reference compound, respectively.

The superoxide anion radical $O_2^{\bullet-}$ generation was evaluated using standard formazan assay.[35] The cuvette was filled with 2 mL of bidistilled water (p*H* = 6.5), containing NADH (0.4 mM), NBT (48 μM), EDTA (20 μM) and compound under study in the form of PVP-based nanoparticles. The cuvette with the solution was illuminated with the described above setup with the LEDs (λ = = 660 nm, radiation power = 70 mW). The optical density of formazan was measured every 1 minute of light exposure at 560 nm. Relative efficiency of superoxide generation was calculated according to a formula similar to formula (2), reaction rate constant for aluminum phthalocyanine chloride was taken as one. All measurements of reactive oxygen species (ROS) generation were carried out at least three times for each compound under study.

Results and Discussion

Characterization of reaction products

The MALDI-TOF mass spectra of the dyads show peaks of molecular ions corresponding to the C_{60}-R-COO-AlPc structure of dyad **III** (negative ions, Figure 2) and dyad **IV** (positive ions, Figure 3). The rest of the peaks belong to different fragments of this structure. For example, in the spectrum of dyad **III**, the peak at 895 Da corresponds to the fullerene derivative **I**, and the peak at 850 Da corresponds to the product of its decarboxylation. In the spectrum of dyad **IV**, the intense peak at 717 Da corresponds to the fullerene derivative **II** elimination product, ylide, coordinated to aluminum phthalocyanine. The fragmentation of fullerene derivatives under the conditions of a mass spectrometric experiment is well-known and leads to the formation of free C_{60} as a thermodynamically stable product as well as addends in the form of unstable ions and radical ions.[36] For example, it is known that pyrrolidinofullerenes decompose to ylides during the ionization process.[37] Separately should mention the peak at 1310 Da, which presumably refers to the oxidation product of the aluminum phthalocyanine in the dyad (Figure 3, inset B).

Absorption and fluorescence spectra

Similarly to the synthesis described above (Figure 1), a supramolecular dyad composed of a fullerene derivative **II** and aluminum naphthalocyanine was also obtained. The dyad NcAl-C_{60} showed an intensive absorption peak at 792 nm in pyridine. Unfortunately, that absorbance peak completely disappeared within less than an hour after the synthesis of the dyad (Figure 4). We believe that rapid post-synthetic destruction of the dyad was caused, most likely, by a significant increase in autoxidation processes due to the influence of the fullerene core.

Apparently, all naphthalocyanine–fullerene dyads have such low stability. To the best of our knowledge, no works on the synthesis and study of the properties of covalently bonded naphthalocyanine–fullerene structures have been published so far. There are only a few works where the naphthalocyanine–fullerene dyads were studied.[38,39] These dyads were based on the coordination complexes of zinc naphthalocyanine and fullerene derivatives containing pyridine or imidazole fragments capable of coordinating to the zinc ion. However, even these dyads have not been isolated and characterized by structural analysis methods (*i.e.*, NMR).

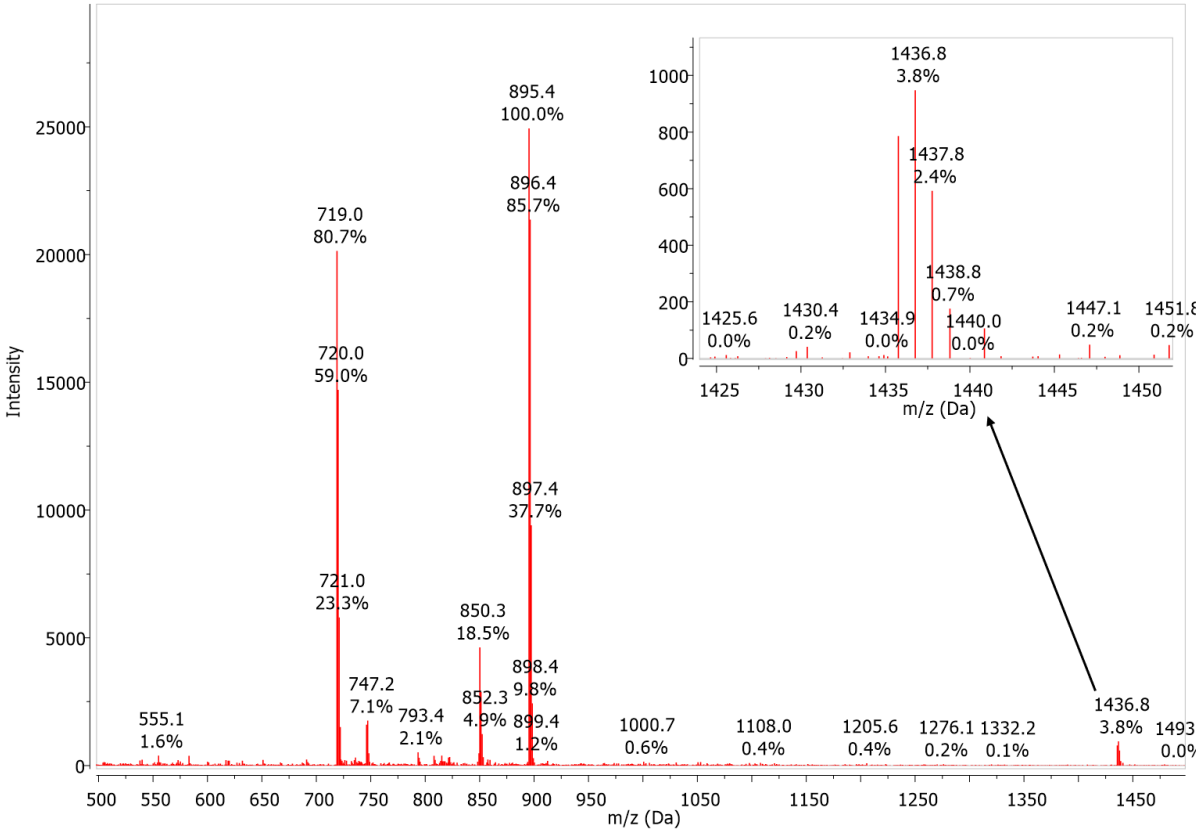

Figure 2. MALDI TOF mass spectrum (negative ion mode, DHB matrix) of dyad **III** and its isotopic pattern (inset).

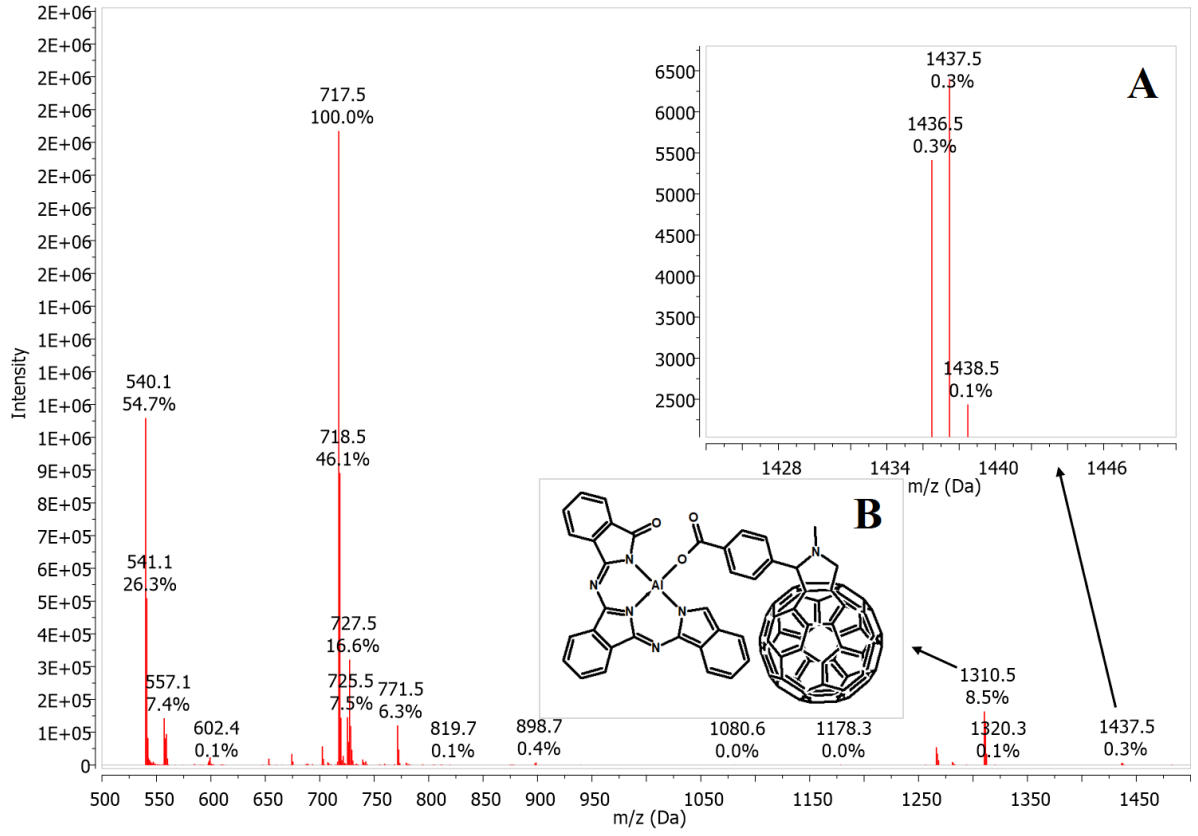

Figure 3. MALDI TOF mass spectrum (positive ion mode, DHB matrix) of dyad **IV**, its isotopic pattern (inset A) and oxidation product of the dyad **IV** (inset B).

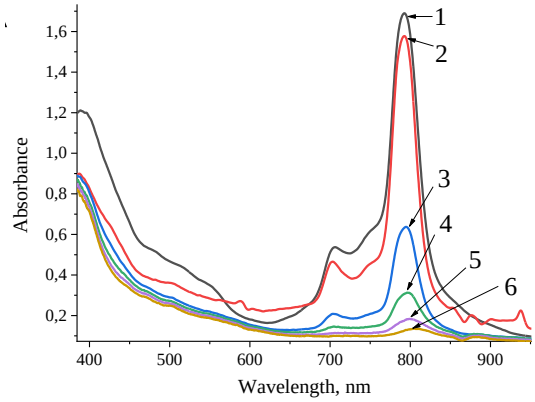

Figure 4. Absorbance spectra of aluminum naphthalocyanine (1) and supramolecular dyad NcAl–C_{60} right after the synthesis (2), after 2 min (3), 5 min (4), 7 min (5), 15 min (6) of incubation in pyridine at room temperature.

The absorption spectra of **PcAl** and supramolecular dyads **III** and **IV** in pyridine are shown in Figure 5,A. The native dye **PcAl** has a characteristic Q-band with an absorption maximum at 677 nm in pyridine. The attachment of fullerene derivatives to **PcAl** by extracoordination has practically no effect on the shape and position of the Q-band maximum, except for slight differences in the region of its vibrational satellites. Due to the low solubility of **PcAl** in pyridine, its concentration was additionally determined from the known extinction coefficient (log ε_{676} = 5.31 in DMF[28]). The solubility of supramolecular dyads **III** and **IV** in pyridine significantly exceeds the solubility of the native dye **PcAl**. We attribute this to the influence of the large extra ligand (fullerene derivative) which prevents the aggregation of phthalocyanines. The determined extinction coefficients for dyads **III** and **IV** in pyridine (log ε_{677} = 4.87, log ε_{678} = 5.0 respectively) turned out to be slightly lower than the extinction coefficient for the native dye (Table 1).

There is no significant change in either the shape of the fluorescence spectra of dyads or the position of its maximum compared to the native dye (Figure 5,B). As can be seen from Table 1, the fluorescence of aluminum phthalocyanine moiety in the dyads is only partially quenched. The fluorescence quantum yield decreased by 1.5 times for dyad **III** and 1.2 times for dyad **IV** relative to that for **PcAl**.

Absorbance and DLS spectra of the dyads encapsulated in PVP nanoparticles

In order to study the generation of superoxide in an aqueous solution, the obtained compounds were incorporated into nanoparticles based on polyvinylpyrrolidone. The size of nanoparticles was estimated using the DLS method (Figure 6). **PcAl-PVP** nanoparticles had a bimodal distribution of average hydrodynamic radius (R_h 3–11 and 50–105 nm). Dyad **IV-PVP** had a wider distribution with R_h 3-5, 15-30 and 50-105 nm. The widest size distribution was observed for dyad **III-PVP** (R_h from 2 to 70 nm). The differences in the sizes of nanoparticles of the dyads **III-PVP** and **IV-PVP** could be related to the different conformation mobility of their linkers between the dye and fullerene core: dyad **III** has the most labile linker of the saturated hydrocarbon chain while dyad **IV** has much more rigid linker with phenol ring (Figure 1). Such mobility, in turn, could have a significant influence on the aggregation processes of the dyads, encapsulated in PVP nanoparticles and, ultimately, size distribution of nanoparticles.

As can be seen from the absorption spectra of aqueous solutions of nanoparticles (Figure 7), aluminum phthalocyanine has a tendency to aggregate in the case of both native dye and supramolecular dyads. A second absorption band appears at 641 nm, which, most likely, belongs to the μ-oxodimers of the PcAl-O-PcAl type.

Table 1. Photophysical and photochemical properties of supramolecular dyads **III** and **IV** and native dye **PcAl**.

	PcAl	Dyad **III**	Dyad **IV**
Absorbance λ_{max}, nm	676[a]	677	678
log(ε) at λ_{max}, M^{-1} cm^{-1}	5.31[a]	4.87	5.01
Fluorescence λ_{max}, nm	685	685	686
Φ_f[b], %	63.3	41.9	54.5
Φ_Δ[c] (mean±SD), %	35.3±4.3	17.2±3.7	21.5±1.4
Relative efficiency of super-oxide generation in water, a.u.	1.0	3.0	0.6

[a]Solvent – DMF, pyridine was used for other measurements unless otherwise noted
[b]Chlorin e_6 trisodium salt was used as a reference (Φfl = 15% in ethanol[32])
[c]Zinc phthalocyanine was used as a reference (Φ_Δ = 40% in DMSO[34])

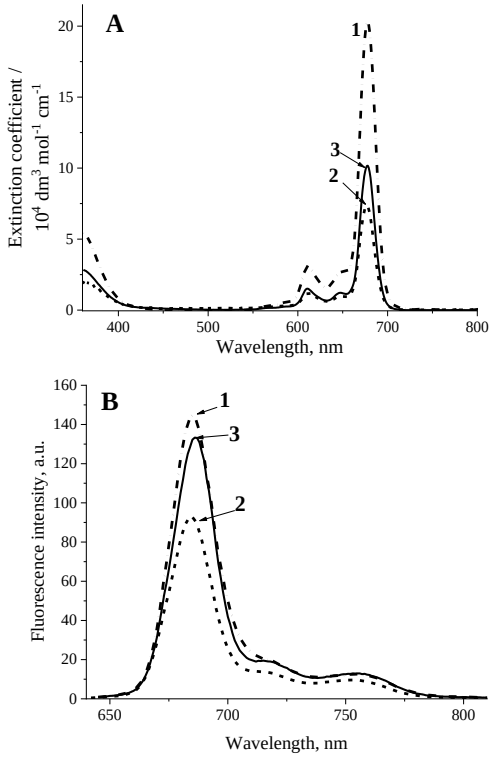

Figure 5. Absorption (A) and fluorescence (B) spectra of **PcAl** (1), dyads **III** (2) и **IV** (3) in pyridine. Fluorescence intensity was corrected on the absorbance at λ_{ex} = 630 nm.

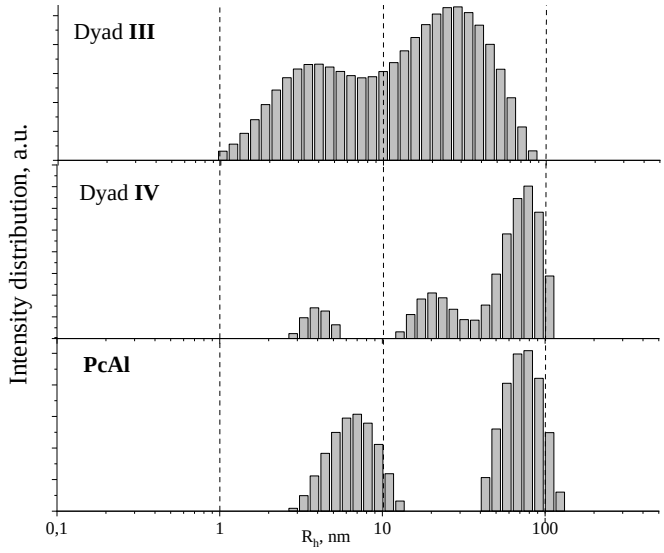

Figure 6. DLS profiles of aqueous solutions of compounds under study, encapsulated in PVP nanoparticles. The concentration of the compounds – 10 μM.

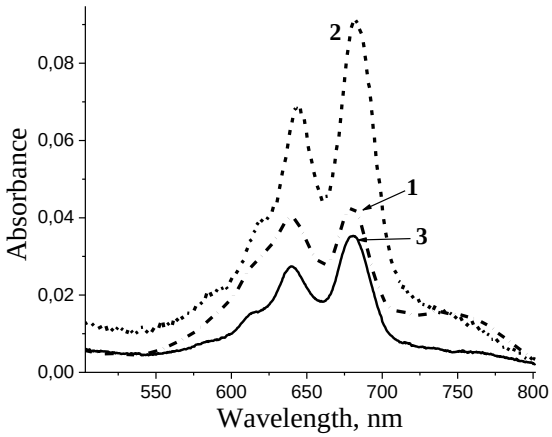

Figure 7. Absorption spectra of aqueous solutions of **PcAl** 2 μM (1); dyad **III** 5 μM (2); dyad **IV** 2 μM (3) encapsulated in PVP nanoparticles.

Photogeneration of reactive oxygen species

The generation of singlet oxygen was studied in pyridine using the 1,3-diphenylisobenzofuran (DPBF) as a probe (Figure 8,A), singlet oxygen quantum yield Φ_Δ was calculated according to formula (2) for all compounds under study (Table 1). A decrease in singlet oxygen generation efficiency is observed in all dyads compared to the native dye. The observed effect could be explained by the influence of the fullerene core of the dyads, which increases the contribution of other energy relaxation pathways of the photoexcited dye moiety. Furthermore, as in the case of the fluorescence quantum yield, this effect is more pronounced for dyad **III**: the value of Φ_Δ was two times lower compared to **PcAl** (17.2% and 35.3%, respectively, Table 1); the efficiency of dyad **IV** was 1.6 times less (21.5%, Table 1). It could also be explained by the different conformation mobility of their linkers between the dye and fullerene core of the dyads, as discussed above.

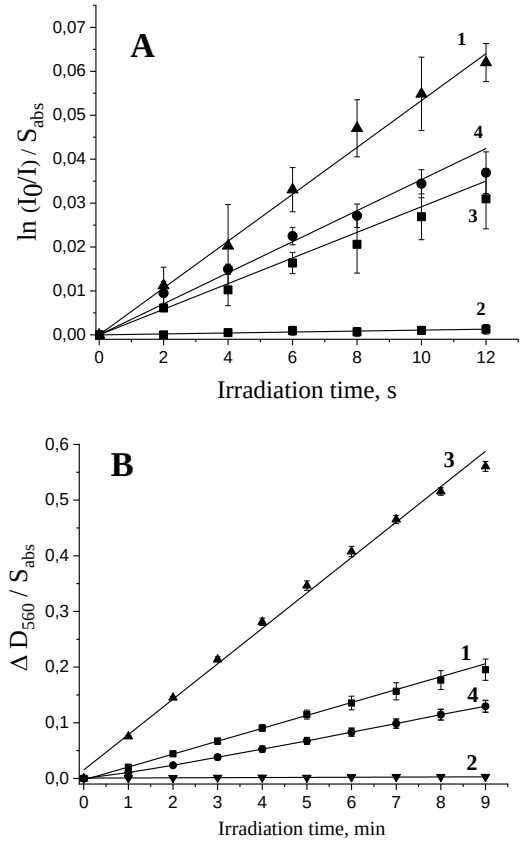

Figure 8. Kinetics of singlet oxygen generation in pyridine (A) and superoxide generation in PVP nanoparticles, water solution (B) of compounds: native dye **PcAl** (1), control (2), and dyads **III** (3) and **IV** (4).

The rate of superoxide photogeneration was measured in an aqueous solution of PVP-based nanoparticles (Figure 8, B). The generation efficiency was evaluated relative to nanoparticles with **PcAl** (Table 1). For supramolecular dyad **IV**, the efficiency of superoxide generation decreased compared to the native dye by 1.67 times, which is similar to a decrease in singlet oxygen generation (Figure 8,A and Table 1). Apparently, in that dyad, electron transfer from aluminum phthalocyanine to fullerene derivative **II** is significantly hampered, and the most part of the photoexcitation energy of the dye dissipates to the heat via relaxation pathways. It leads to a decrease in both the quantum yield of triplet formation for aluminum phthalocyanine moiety, which reduces the singlet oxygen production, and the efficiency of electron transfer from the dye to fullerene, which, in turn, reduces the superoxide generation efficiency of the dyad.

The superoxide generation efficiency of dyad **III**, on the contrary, increased by 3 times compared to the native dye **PcAl**. Facilitated electron transfer from the dye to the fullerene can be explained both by the higher conformation mobility of the linker and by the higher electron affinity of the fullerene derivative **I** compared to derivative **II**. The LUMO energy level of -4.17 eV was estimated for $PC_{60}BM$ (a compound with a similar chemical structure to fullerene derivative **I**) by the method of cyclic voltammetry *versus* the Fc^+/Fc redox couple in work,[40] while fullerene derivative **II** has higher LUMO level of -3.91 eV, which was calculated by the same method.[41]

Conclusion

Using the ability of aluminium ion in the centre of the phthalocyanine macrocycle to bear an axial ligand, we obtained supramolecular dyads **III** and **IV** based on aluminum phthalocyanine and fullerene C_{60} derivatives. Compared to the native dye, the fluorescence in the obtained dyads is partially quenched and the singlet oxygen generation ability is reduced. Dyad **III** based on phenyl-C_{60}-butyric acid and encapsulated in polyvinylpyrrolidone nanoparticles showed a threefold increase in in the superoxide anion-radical generation compared to the native dye. These results suggest the effective formation of the charge transfer state in this dyad. This makes dyad **III** worthy of attention in the further development of Type I photosensitizers for PDT. Also, the applied approach could be useful tool for the quick screening dye–fullerene donor-acceptor pairs and the directed search of the most effective ones.

Acknowledgements. The synthesis and analysis of dyad **III** were financially supported by president grant No. MK-4079.2021.1.4. The synthesis and analysis of dyad **IV** were financially supported by the Russian Science Foundation (Grant No. 20-74-00107). Analysis of photophysical and photochemical properties of the dyads was performed on equipment of the Biomedical Institute of the Scientific and Educational Center of Moscow Region State University in Chernogolovka.

References

1. Mroz P., Pawlak A., Satti M., Lee H., Wharton T., Gali H., Sarna T., Hamblin M.R. *Free Radical Bio. Med.* **2007**, *43*, 711–719.
2. Chen D., Xu Q., Wang W., Shao J., Huang W., Dong X. *Small* **2021**, *17*, 2006742.
3. Wang Y.Y., Liu Y.C., Sun H.W., Guo D.S. *Coord. Chem. Rev*. **2019**, *395*, 46–62.
4. Li Y., Zhang W., Niu J., Chen Y. *Am. Chem. Soc. Nano* **2012**, *6*, 5164−5173.
5. Zheng D.W., Li B., Li C.X., Fan J.X., Lei Q., Li C., Xu Z., Zhang X.Z. *Am. Chem. Soc. Nano* **2016**, *10*, 8715−8722.
6. Ding H., Yu H., Dong Y., Tian R., Huang G., Boothman D.A., Sumer B.D., Gao J. *J. Control. Release* **2011**, *156*, 276−280.
7. Lan G., Ni K., Veroneau S.S., Feng X., Nash G.T., Luo T., Xu Z., Lin W. *J. Am. Chem. Soc.* **2019**, *141*, 4204−4208.
8. Li Q., Huang C., Liu L., Hu R., Qu J. *Cytometry* **2018**, *93*, 997–1003.
9. Ohkubo K., Fukuzumi S. *Bull. Chem. Soc. Jap.* **2009**, *82*, 303–315.
10. Milanesio M.E., Alvarez M.G., Rivarola V., Silber J.J., Durantini E.N. *Photochem. Photobiol.* **2005**, *81*, 891–897.
11. Belik A.Y., Rybkin A.Y., Voronov I.I., Goryachev N.S., Volyniuk D., Grazulevicius J.V., Troshin P.A., Kotelnikov A.I. *Dyes Pigm*. **2017**, *139*, 65–72.
12. Kotelnikov A.I., Rybkin A.Y., Khakina E.A., Kornev A.B., Barinov A.V., Goryachev N.S., Ivanchikhina A.V., Peregudov A.S., Martynenko V.M., Troshin P.A. *Org. Biomol. Chem*. **2013**, *11*, 4397.
13. Rybkin A.Y., Belik A.Y., Tarakanov P.A., Taziev K.R., Kozlov A.V., Goryachev N.S., Sulimenkov I.V., Kozlovskiy V.I., Romanenko Y.V., Koifman O.I., Kotelnikov A.I. *Macroheterocycles* **2019**, *12*, 181–186.
14. Rybkin A.Y., Belik A.Y., Goryachev N.S., Mikhaylov P.A., Kraevaya O.A., Filatova N.V., Parkhomenko I.I., Peregudov A.S., Terent'ev A.A., Larkina E.A., Mironov A.F., Troshin P.A., Kotelnikov A.I. *Dyes Pigm*. **2020**, *180*, 108411.
15. Miller J.D., Baron E.D., Scull H., Hsia A., Berlin J.C., McCormick T., Colussi V., Kenney M.E., Cooper K.D., Oleinick N.L. *Toxicol. Appl. Pharm*. **2007**, *224*, 290–299.
16. Jiang Z., Shao J., Yang T., Wang J., Jia L. *J. Pharmaceut. Biomed. Anal.* **2014**, *87*, 98–104.
17. Tedesco A., Rotta J., Lunardi C.N. *Curr. Org. Chem*. **2003**, *7*, 187–196.
18. Koifman O.I., Ageeva T.A., Beletskaya I.P., Averin A.D., Yakushev A.A., Tomilova L.G.,.Dubinina T.V., Tsivadze A.Yu., Gorbunova Yu.G., Martynov A.G., Konarev D.V., Khasanov S.S., Lyubovskaya R.N., Lomova T.N., Korolev V.V., Zenkevich E.I., Blaudeck T. , Ch. von Borczyskowski, Zahn D.R.T., Mironov A.F., Bragina N.A., Ezhov A.V., Zhdanova K.A., Stuzhin P.A., Pakhomov G.L., Rusakova N.V., Semenishyn N.N., Smola S.S., Parfenyuk V.I., Vashurin A.S., Makarov S.V., Dereven'kov I.A., Mamardashvili N.Zh., Kurtikyan T.S., Martirosyan G.G., Burmistrov V.A., Aleksandriiskii V.V., Novikov I.V., Pritmov D.A., Grin M.A., Suvorov N.V., Tsigankov A.A., Fedorov A.Yu., Kuzmina N.S., Nyuchev A.V., Otvagin V.F., Kustov A.V., Belykh D.V., Berezin D.B., Solovieva A.B., Timashev P.S., Milaeva E.R., Gracheva Yu.A., Dodokhova M.A., Safronenko A.V., Shpakovsky D.B., Syrbu S.A., Gubarev Yu.A., Kiselev A.N., Koifman M.O., Lebedeva N.Sh., Yurina E.S. *Macroheterocycles* **2020**, *13*, 311–467.
19. Bottari G., Trukhina O., Ince M., Torres T. *Coord. Chem. Rev*. **2012**, *256*, 2453–2477.
20. Troshin P.A., Koeppe R., Peregudov A.S., Peregudova S.M., Egginger M., Lyubovskaya R.N., Sariciftci N.S. *Chem. Mater*. **2007**, *19*, 5363–5372.
21. D'Souza F., Maligaspe E.. Ohkubo K., Zandler M.E., Subbaiyan N.K., Fukuzumi S. *J. Am. Chem. Soc.* **2009**, *131*, 8787–8797.
22. Rio Y., Seitz W., Gouloumis A., Vázquez P., Sessler J.L., Guldi D.M., Torres T. *Chem.–Eur. J.* **2010**, *16*, 1929–1940.
23. Das S.K., Mahler A., Wilson A.K., D'Souza F. *ChemPhysChem* **2014**, *15*, 2462–2472.
24. Chen X.-F., El-Khouly M.E., Ohkubo K., Fukuzumi S., Ng D.K.P. *Chem.–Eur. J.* **2018**, *24*, 3862–3872.
25. Ballesteros B., Torre G., Torres T., Hug G.L., Rahman G.M., Guldi D.M. *Tetrahedron* **2006**, *62*, 2097–2101.
26. Martín-Gomis L., Ohkubo K., Fernández-Lázaro F., Fukuzumi S., Sastre-Santos A. *Org. Lett.* **2007**, *9*, 3441–3444.
27. Ovchenkova E.N., Bichan N.G., Ksenofontov A.A., Lomova T.N. *J. Fluorine Chem*. **2019**, *224*, 113–120.
28. Ogunsipe A., Opeolu S. *Chem. Res. J.* **2020**, *5*(3), 136–143.
29. Hummelen J.C., Knight B.W., LePeq F., Wudl F., Yao J., Wilkins C.L. *J. Org. Chem*. **1995**, *60*, 532–538.
30. Hau S.K., Cheng Y-J., Yip H-L., Zhang Y., Ma H., Jen AK-Y. *ACS Appl. Mater. Inter*. **2010**, *2*, 1892–1902.
31. Yamakoshi Y.N., Yagami T., Fukuhara K., Sueyoshi S., Miyata N. *J. Chem. Soc. Chem. Commun.* **1994**, *1*, 517–518.
32. Zenkevich E., Sagun E., Knyukshto V., Shulga A., Mironov A., Efremova O., Bonnett R., Pinda Songca S., Kassem M. *J. Photochem. Photobiol. B* **1996**, 33, 171–180.
33. Wang P., Qin F., Zhang Z., Cao W. *Optics Express* **2015**, *23*, 22991–23003.
34. Zhang X-F., Xu H. *J. Chem. Soc. Faraday Trans*. **1993**, *89*, 3347–3351.
35. Yamakoshi Y., Umezawa N., Ryu A., Arakane K., Miyata N., Goda Y., Masumizu T., Nagano T. *J. Am. Chem. Soc.* **2003**, *125*, 12803–12809.
36. Markov V.Y., Borschevsky A.Y., Sidorov L.N. *Int. J. Mass Spectrom*. **2012**, *325–327*, 100–112.
37. Delgado J.L., Filippone S., Martín-Domenech A., Altable M., Maroto E., Langa F., Martín N., Martínez-Alvarez R. *J. Am.*

Chem. Soc. Mass Spectrom. **2011**, *22*, 557–567.
38. El-Khouly M.E., Rogers L.M., Zandler M.E., Suresh G., Fujitsuka M., Ito O., D'Souza F. *ChemPhysChem* **2003**, *4*, 474–481.
39. Zandler M.E., D'Souza F. *Comptes Rendus Chimie* **2006**, *9*, 960–981.
40. Mumyatov A.V., Goryachev A.E., Prudnov F.A., Mukhacheva O.A., Sagdullina D.K., Chernyak A.V., Troyanov S.I., Troshin P.A. *Synthetic Met.* **2020**, *270*, 116565.
41. Kozlov A.V., Rybkin A.Y., Belik A.Y., Kostina E.A., Goryachev N.S., Sulimenkov I.V., Kozlovskiy V.I., Istakova O.I., Konev D.V., Kotelnikov A.I. *Mendeleev Commun.* **2021**, *31*, 807–809.

Received 16.12.2022
Accepted 20.02.2023